NeuroImage **13,** 196–209 (2001)
doi:10.1006/nimg.2000.0659, available online at http://www.idealibrary.com on IDEAL®

# Location-Probability Profiles for the Mouth Region of Human Primary Motor–Sensory Cortex: Model and Validation

Peter T. Fox, Aileen Huang, Lawrence M. Parsons, Jin-Hu Xiong, Frank Zamarippa, Lacy Rainey, and Jack L. Lancaster

*Research Imaging Center, University of Texas Health Science Center at San Antonio, San Antonio, Texas*

Received May 15, 2000; published online November 15, 2000

**The mouth representation of the human, primary motor cortex (M1) is not reliably identified by surface anatomy but may be reliably localized by means of spatial coordinates. For this report, three quantitative metanalyses were performed which jointly described the mean location, location variability and location-probability profiles of the human M1-mouth representation. First, a literature metanalysis of intersubject functional-area variability was performed using eleven, per-subject studies, each of which reported a coordinate-referenced measure of intersubject variability for one or more brain areas. From these data, a weighted-mean value for intersubject variability was computed, which proved to be small (5.6 mm, standard deviation), consistent across coordinate axes (x, y, z), and consistent across brain areas. Second, a literature metanalysis of the location of M1-mouth was performed using seven, coordinate-referenced, group-mean studies (71 subjects in all), each of which reported a grand-average location for M1-mouth. From this, a weighted-mean location and weighted values for total variability (interlaboratory plus interindividual) were determined. Using these two literature metanalyses as input data, location-probability profiles were computed for the cardinal axes (x, y, and z) of the reference space, using the functional volumes modeling (FVM) statistical model. Third, an original-data metanalysis was performed on in-house PET data from 30 normal subjects performing overt-speech tasks. M1-mouth's mean location, location variability, and location-probability profiles were consistent with those conjointly modeled by FVM from the two literature metanalyses. Collectively, these observations provide a detailed, consensus probabilistic description of the location of the human M1-mouth representation in standardized coordinates.** © 2001 Academic Press

***Key Words:*** **M1; primary motor; individual variability; mouth; cortex; PET.**

The purpose of the present study was to define in quantitative terms the location and location variability of the mouth representation of human primary motor cortex (M1), based upon noninvasive, functional neuroimaging. In qualitative terms, the location of M1 is well known: it lies on the posterior bank of the precentral gyrus, bounded posteriorly by the pit of the central sulcus and anteriorly by the crown of the pre-central gyrus (Zilles *et al.*, 1995). M1's internal organization is somatotopic, following the now-classical homuncular pattern originally illustrated by Woolsey (1952) and Penfield (1950), wherein the mouth representation is perisylvian, the foot representation faces the interhemispheric fissure, and the hand representation lies roughly midway between. Despite the apparent simplicity and reliability of this structure–function correspondence, noninvasive identification of M1 by surface anatomy is remarkably problematic and especially so for the face representation, for several reasons. First, despite their relative prominence, the central sulcus and the precentral gryus are not reliably identified by visual inspection. Sobel *et al.* (1993) reported only 50% agreement among experts (neuroradiologists) in identifying the central sulcus within magnetic resonance images (MRI). Similarly, neurosurgeons routinely use cortical electrical stimulation and recording to identify the central sulcus, and do not rely on visual landmark identification (Goldring, 1978). Second, while M1 is reliably bounded posteriorly, no comparably reliable landmarks exist for the anterior, superior, or inferior borders. Individual variability in M1 borders led Brodmann to a conjecture, which foreshadowed the development of probabilistic descriptions of brain structural and functional boundaries, stating: "the rostral border . . . is rather unclear and variable, . . . and can only be determined from numerous individual brains" (Garey, 1994). Third, the functional segregation of Brodmann area 4 (BA4) into a motor homonculus lacks any clear boundaries or landmarks. Thus, even if the primary motor area were readily identified, its functional parcellation would not be. Fourth, the sulcal anatomy of the frontal operculum, including the inferior aspect of the central sulcus is particularly vari-



1053-8119/01 $35.00

able, presumably undermining reliable structure–function correspondences (Ono *et al.,* 1990; Garey, 1994). Collectively, then, it is not surprising that Grafton *et al.* (1991) found that the M1 mouth representation "was identified by no sulcus or other surface landmark," when coregistering PET activations onto 3-D-rendered MRI's.

Standardized coordinates offer an alternative to surface landmarks for describing the locations of functional areas within the brain (Fox *et al.,* 1985, 1997). The literature adhering to this reporting standard is now quite large (Fox, 1995b, 1998). However, the great majority of the coordinate-referenced, brain-mapping literature reports only group-mean locations, absent any measure of intersubject variability. Less than a dozen studies have reported intersubject variability of functional areas in standardized coordinates (Table 1, below). Despite this paucity of coordinate-referenced studies of intersubject variability, overall, they suggest that intersubject variability is sufficiently low that probabilistic models of brain functional areas should be reasonably precise and potentially useful (Table 1, below). Prospective, empirical construction of spatial probability contours for functional areas is a formidable undertaking. Accurate and precise probability bounds would likely require scores or even hundreds of subjects for each brain area. This assumes, of course, that tasks suitable for activating specific functional areas on a per-subject basis are available. An alternative is to retrospectively develop spatial probability bounds through metanalysis of the coordinate-referenced literature. The shortage of studies directly addressing individual variability is an impediment for which a solution has been proposed. A method of modeling spatial probability contours for brain functional areas using both group-mean studies (to provide a weighted-mean location and intergroup variability) and per-subject studies (to provide an estimate of intersubject variability) has been reported (Fox *et al.,* 1997). In the present report, this method (called functional volumes modeling or FVM) was used to model spatial-probability contours for the M1 mouth representation. In parallel, spatial probability contours for M1 mouth were determined from an original-data metanalysis of 30 normal volunteers, possibly the largest, coordinate-referenced report of the intersubject variability of any functional area. Jointly, these two metanalyses were used to model the location, variability and spatial probability profiles of M1 mouth.

## METHODS

*Literature metanalysis of intersubject variability.* Intersubject variability in the location of brain functional areas was estimated from the literature reporting per-subject response coordinates from any brain area. A total of 514 variability values were obtained from 11 peer-reviewed studies (Fox *et al.,* 1985a, c, 1987b, a; Belliveau *et al.,* 1991; Grafton *et al.,* 1993; Watson *et al.,* 1993; Schneider *et al.,* 1994; Hunton *et al.,* 1996; Ramsey *et al.,* 1996; Hasnain *et al.,* 1998), which collectively reported on more than 40 functional areas which were imaged in over 100 subjects (Table 1). Sample sizes ranged from 2 to 21. No paper reported the location variability of the M1 mouth representation. One paper (Fox *et al.,* 1987a) reported the variability of the primary sensory (S1) mouth representation, using vibrotactile stimulation as the provocation. Five papers reported the variability of the M1 or S1 hand representation (Fox *et al.,* 1985, 1987a; Grafton *et al.,* 1993; Hunton *et al.,* 1996; Ramsey *et al.,* 1996). The remaining six sources of individual-variability estimates were from locations further removed from M1-mouth. For the most part, variability values were reported in millimeter standard deviations following size normalization to Talairach and Tournoux (1988). If otherwise expressed, values were converted to these units prior to analysis. From these 11 papers, the pooled variance (weighted per-location by $n$) was computed and reported as the standard deviation for each axis (x, y, z) (Table 1). This value was used as an input parameter for FVM modeling of the spatial-probability profiles of M1-mouth (below).

*Literature metanalysis of M1-mouth and functional volume modeling.* The mean location and total variability (interlaboratory plus intersubject) of M1-mouth were estimated from the coordinate-referenced, group-mean, brain-activation literature. Candidate studies were limited to those: (1) on normal subjects; (2) using overt oral tasks. Eight such studies were identified (Petersen *et al.,* 1988; Paus *et al.,* 1993; Petrides *et al.,* 1993; Andreasen *et al.,* 1995; Bookheimer *et al.,* 1995; Fox *et al.,* 1996; Braun *et al.,* 1997; Murphy *et al.,* 1997). Of these, one (Fox *et al.,* 1996) was discarded because the subject sample partially overlapped the sample of the present original-data metanalysis (below). Two (Andreasen *et al.,* 1995; Murphy *et al.,* 1997) were discarded because they failed to differentiate between M1-mouth and ventral premotor cortex (i.e., BA 6/44 or Broca's area). Ventral premotor cortex lies approximately 2 cm inferior to M1-mouth and is activated during covert tasks, such as imagined movements (Fox, 1995a; Parsons and Fox, 1998), as well as by overt tasks such as actual speech or other movements (Petersen *et al.,* 1988; Paus *et al.,* 1993; Petrides *et al.,* 1993; Bookheimer *et al.,* 1995; Fox *et al.,* 1996; Braun *et al.,* 1997). M1-mouth, on the other hand, is not appreciably activated by covert tasks, such as imagined speech. Failure to differentiate these adjacent regions resulted in activation coordinates (Andreasen *et al.,* 1995; Murphy *et al.,* 1997) lying roughly midway between these two, well-defined, functional regions, which would have skewed the metanalysis, if included. No other exclusions were made. In total, five studies ranging in group-size ($n$) from 8 to 20 and totaling 71

**TABLE 1**

Variability Input Data

| Citation | Functional area | *n* | Standard deviations | | |
|---|---|---|---|---|---|
| | | | X axis | Y axis | Z axis |
| Fox *et al.*, 1985a | SMA hand (m) | 9 | 9.60 | 7.00 | 9.40 |
| | FEF (l) | 9 | 9.40 | 7.50 | 7.40 |
| | FEF (r) | 9 | 12.00 | 6.80 | 8.60 |
| | M1 hand (l) | 9 | 4.40 | 7.40 | 6.30 |
| | M1 hand (r) | 9 | 7.30 | 3.20 | 6.50 |
| | V1 (m) | 9 | 5.30 | 5.10 | 8.90 |
| Fox *et al.*, 1985c | Ant Cbm eye (m) | 7 | 4.00 | 6.00 | 6.00 |
| | Ant Cbm hand (l) | 15 | 5.00 | 4.00 | 5.00 |
| | Ant Cbm hand (r) | 15 | 6.00 | 5.00 | 5.00 |
| Fox *et al.*, 1987b | V1 0.1–1.5 deg (m) | 5 | — | 1.3 | 3.6 |
| | V1 1.5–5.5 deg (m) | 6 | — | 0.9 | 3.2 |
| | V1 5.5–15.5 deg (m) | 6 | — | 0.7 | 4.2 |
| Fox *et al.*, 1987a | S1 lip (l) | 7 | 3.64 | 4.59 | 7.44 |
| | S1 lip (r) | 7 | 4.40 | 4.90 | 6.00 |
| | S1 hand (l) | 8 | 4.90 | 5.60 | 1.90 |
| | S1 hand (r) | 8 | 3.74 | 5.88 | 2.60 |
| | S1 foot (m) | 8 | 5.18 | 10.70 | 3.70 |
| Belliveau *et al.*, 1991 | V1 0–90 deg (l) | 7 | 2.00 | 5.00 | 5.00 |
| | V1 0–90 deg (r) | 7 | 2.00 | 5.00 | 4.00 |
| Grafton *et al.*, 1992 | M1 shoulder (l) | 4 | 2.00 | 4.00 | 2.00 |
| | M1 elbow (l) | 4 | 4.00 | 7.00 | 4.00 |
| | M1 wrist (l) | 4 | 4.00 | 2.00 | 5.00 |
| | M1 finger (l) | 6 | 8.00 | 8.00 | 8.00 |
| | CMA shoulder (l) | 4 | 2.00 | 3.00 | 6.00 |
| | CMA elbow (l) | 4 | 2.00 | 3.00 | 8.00 |
| | CMA wrist (l) | 4 | 2.00 | 5.00 | 8.00 |
| | CMA finger (l) | 6 | 4.00 | 6.00 | 5.00 |
| | Ant Cbm shoulder (l) | 4 | 6.00 | 7.00 | 3.00 |
| | Ant Cbm elbow (l) | 4 | 7.00 | 9.00 | 4.00 |
| | Ant Cbm wrist (l) | 4 | 8.00 | 8.00 | 5.00 |
| | Ant Cbm finger (l) | 6 | 13.00 | 11.00 | 5.00 |
| | SMA shoulder (l) | 4 | 3.00 | 6.00 | 7.00 |
| | SMA elbow (l) | 4 | 2.00 | 5.00 | 6.00 |
| | SMA wrist (l) | 4 | 1.00 | 8.00 | 7.00 |
| | SMA finger (l) | 6 | 3.00 | 6.00 | 6.00 |
| Watson *et al.*, 1993 | V5 (l) | 12 | 5.60 | 6.00 | 5.30 |
| | V5 (r) | 12 | 3.70 | 4.70 | 3.20 |
| Schneider *et al.*, 1994 | Calcarine (b) | 6 | 2.80 | 6.00 | 3.60 |
| | Fusiform Lingual (b) | 7 | 6.20 | 2.40 | 2.40 |
| | Superior Occipital (b) | 5 | 2.80 | 3.10 | 3.10 |
| | Superior Lateral (b) | 2 | 3.50 | 1.40 | 1.40 |
| | Superior Medial (b) | 2 | 2.10 | 1.40 | 1.40 |
| Hunton *et al.*, 1996 | Group 1 (mixed*) | 21 | 6.70 | 6.30 | 6.10 |
| | Group 2 (mixed*) | 21 | 7.50 | 7.20 | 6.30 |
| Ramsey *et al.*, 1996 | M1 hand (l) (fMRI) | 9 | 4.50 | 3.20 | 5.50 |
| | M1 hand (l) (PET) | 9 | 5.50 | 4.50 | 5.10 |
| Hasnain *et al.*, 1998 | V1 (l) | 11 | 3.30 | 5.30 | 7.50 |
| | V2v (l) | 11 | 4.20 | 5.10 | 4.90 |
| | V2d (l) | 11 | 4.60 | 4.30 | 8.60 |
| | VP (l) | 11 | 2.00 | 7.60 | 5.10 |
| | V3 (l) | 11 | 5.90 | 5.00 | 7.50 |
| | V3a (l) | 11 | 2.90 | 4.90 | 6.10 |
| | V4 (l) | 11 | 4.50 | 5.00 | 3.60 |
| | V5 (l) | 11 | 4.60 | 3.70 | 3.80 |
| | V1 (r) | 11 | 2.60 | 5.70 | 5.00 |
| | V2v (r) | 11 | 4.00 | 5.90 | 5.90 |
| | V2d (r) | 11 | 3.50 | 4.30 | 4.50 |
| | VP (r) | 11 | 4.40 | 5.70 | 5.40 |
| | V3 (r) | 11 | 5.90 | 5.50 | 4.20 |
| | V3a (r) | 11 | 9.30 | 6.10 | 3.40 |
| | V4 (r) | 11 | 3.30 | 5.60 | 2.90 |
| | V5 (r) | 11 | 4.70 | 7.00 | 6.20 |
| Cumulative *n* | | 514 | | | |
| Weighted-mean standard deviations (mm) | | | 5.47 | 5.75 | 5.64 |

*Note.* Intersubject variability in the coordinate-referenced locations of brain functional areas is shown. A total of 514 variability values were obtained from 11 peer-reviewed studies (Fox *et al.*, 1985a; Fox *et al.*, 1985c; Fox *et al.*, 1987b; Fox *et al.*, 1987a; Belliveau *et al.*, 1991; Grafton *et al.*, 1992; Watson *et al.*, 1993; Schneider *et al.*, 1994; Hunton *et al.*, 1996; Ramsey *et al.*, 1996; Hasnain *et al.*, 1998), which collectively reported on more than 40 functional areas that were imaged in over 100 subjects. Reported variability values are expressed in millimeter standard deviations. Functional areas are designated by area name, map segment, and laterality. Area name abbreviations are: Ant Cbm, anterior cerebellum; CMA, cingulate motor area; FEF, frontal eye fields; M1, primary motor cortex; S1, primary somatosensory cortex; SMA, supplementary motor area; V1, primary visual cortex V2v, V2d, second visual area, ventral and dorsal components; V3, V3a, third visual area; V4, fourth visual area; V5, fifth visual area. Laterality is coded as: l, left; r, right; m, midline; b, both sides.

**TABLE 2**

M1-Mouth Input Data

| Citation | Task | *n* | Left | | | Right | | |
|---|---|---|---|---|---|---|---|---|
| | | | X axis | Y axis | Z axis | X axis | Y axis | Z axis |
| Petersen *et al.*, 1988 | Speech | 17 | −42.8 | −15.1 | 43.6 | 50.3 | −9.9 | 38.3 |
| Paus *et al.*, 1993 | Speech | 8 | −51.0 | −11.0 | 33.0 | 62.0 | −4.0 | 22.0 |
| Petrides *et al.*, 1993 | Speech | 10 | −50.0 | −11.0 | 38.0 | 44.0 | −6.0 | 36.0 |
| Brookheimer *et al.*, 1995 | Speech | 16 | −45.0 | −10.0 | 38.0 | 42.0 | −4.0 | 44.0 |
| Braun *et al.*, 1997 | Speech | 20 | −48.0 | −16.0 | 28.0 | 44.0 | −16.0 | 28.0 |
| | Total | 71 | | | | | | |

The M1-mouth location coordinates reported in five, group-mean, brain-activation studies contrasting overt speech to a nonspeaking condition are shown. Values are reported by number of subjects (*n*), cerebral hemisphere (left, right), and coordinate axis (x, left–right; y, anterior–posterior; z, superior–inferior).

subjects were accepted (Table 2). All studies reported coordinates by reference either to Talairach and Tournoux (1988) or to Talairach *et al.* (1967). Coordinates referenced to the latter were converted to the former. Although reports varied in the sense (+ or −) applied to the right and left hemispheres, this was standardized to right hemisphere being positive. Using these input data and the FVM modeling construct (Fox *et al.*, 1997), location-probability profiles were computed for each axis (x, y, z) and each hemisphere. Probability contours were computed for the 50th ($z = 0.67$), 68th ($z = 1.0$), and 95th ($z = 1.96$) percentiles along each axis (x, y, and z). These predictions were tested by comparison to an original-data metanalysis of M1-mouth (below). In addition, a summary FVM was constructed using both the literature metanalysis and the original-data metanalysis (Table 5, below).

*Original-data metanalysis of M1-mouth.* The M1-mouth location, variability and spatial-probability profile were determined for each hemisphere and each cardinal axis (x, y, z) from an original-data metanalysis on thirty subjects. Each of the 30 subjects participated in one of three speech-motor protocols (ten subjects per protocol) in the authors' laboratory. All three protocols were designed to allow per-subject identification of speech-motor activations, applying intrasubject image averaging to multiple trials of each condition, to enhance signal-to-noise ratio. In addition, each subject performed at least two different speech motor conditions, which were pooled for the present analysis, further enhancing the detection and localization of the M1-mouth responses.

*Experimental subjects.* All subjects were healthy, right-handed, native English speakers between the ages of 21 and 49 (mean = 32; SD = 7). Cohort One was ten men. Cohorts Two and Three each consisted of five men and five women.

*Behavioral conditions.* Two Cohorts performed two overt speech tasks and one control task, while the third Cohort performed three overt speech tasks and one control task. Cohort One's speech tasks were: (1) reading aloud paragraphs presented on a computer monitor; and (2) paragraph reading while hearing the same paragraph read aloud through an ear phone (Fox *et al.*, 1996). Cohort Two's speech tasks were: (1) speaking aloud a verb in response to a visually presented noun; and (2) naming a visually presented object (a line-drawn picture). Cohort Three's speech tasks were: (1) reading aloud a verb in response to a visually presented noun (same as condition 1 for Cohort 2); (2) speaking aloud a noun (a name) in response to a visually presented object (same stimuli as for Cohort 2, Task 2); and (3) speaking aloud a noun in response to visually presented noun (reading aloud). In Cohorts 1 and 2, each condition was performed three times per subject, in a single scanning session. In Cohort 3, each condition was performed two times per subject. For each subject, all six speech trials were grouped, thereby increasing the signal-to-noise ratio to a level permitting M1-mouth (and other speech-motor responses) to be detected in a high percentage of subjects (80%–93%, below). For all three Cohorts, the control state was fixation-point rest.

*Head fixation and alignment.* For all studies, the head was immobilized in a closely fitted, thermally molded, plastic facial mask that was individually made for each subject (Fox, 1985b). The mask minimized head movement during PET imaging, even during overt speech. The imaging volume exceeded brain size in the x (medial-to-lateral) and y (anterior-to-posterior) axes. In the z-axis (superior to inferior), the field-of-view was 10 cm. In all subjects this volume was angled approximately 10° clockwise (when viewed from the subject's left) from the canthomeatal line, with the lower bound of the imaging volume approximately 1 cm above the tragus. This positioning typically sampled the entire frontal lobe and, in all cases, amply spanned the primary motor area for mouth.

*PET methods.* PET imaging was performed on a GE 4096 camera: pixel spacing = 2.6 mm; spatial res-

olution = 5 mm FWHM; interplane, center-to-center distance = 6.5 mm; scan planes = 15; z-axis field of view = 10 cm. Attenuation correction was performed with a $^{68}Ge/^{68}Ga$ pin source. Brain blood flow (BF) was measured with $H_2{}^{15}O$ (half-life, 123 s), administered as an intravenous bolus of 8–10 ml of saline containing 60 mCi (Raichle *et al.,* 1983; Herscovitch *et al.,* 1983). A 40-s scan was triggered as the tracer bolus entered the field of view (the brain), by the rise in the coincidence-counting rate. As the statistical significance and localization accuracy of functional mapping are not affected by compartmental modeling (Fox *et al.,* 1984; Fox and Mintun, 1989), arterial blood samples were not drawn. A 10-min interscan interval was sufficient for isotope decay (five half-lives) and to reestablish resting-state levels of regional blood flow (rBF) within activated areas. Each condition was imaged three times in each subject. Each PET session lasted approximately 2 h and 30 min. Images were reconstructed using a Hann filter with a width of 5 mm, resulting in images with a spatial resolution of 11.5 mm (full-width at half-maximum).

*Anatomical MRI methods.* Anatomical MRI was acquired in 26 of 30 subjects and used to optimize spatial normalization. MRI imaging was performed on the 1.9-Tesla, Elscint *Prestige* using a high-resolution, 3-D GRASS sequence: TR = 33 ms; TE = 12 ms; flip angle = 60°; voxel size = 1 $mm^3$; matrix size = 256 × 192 × 192; acquisition time = 15 min. Cardiac-gating prevented CSF-pulsation artifacts.

*Image processing.* PET-MRI registration and spatial normalization were performed using the Lancaster *et al.* (1995) algorithm, as implemented in the SN software (Research Imaging Center, UTHSCSA, San Antonio, TX). This algorithm employs a nine-parameter, affine transformation. Images were normalized to the Talairach and Tournoux (1988) atlas and referenced in millimeters relative to the anterior commissure.

Statistical parametric images (SPIs) were created using the Fox *et al.* (1988) algorithm, as implemented in the MIPS software (Research Imaging Center, UTHSCSA). This algorithm uses the pooled variance of all brain voxels as the reference for computing significance, rather than computing the variance at each voxel. This procedure allows formation of a single-subject SPI, even without intrasubject averaging, and is more sensitive for small samples than the voxel-wise variance methods of Friston *et al.* (1991) and others (Strother, 1997). Thirty-one SPIs were created: 30 single-subject SPIs and one 30-subject SPI.

The M1-mouth locations (left and right) were determined in each SPI, as follows. The 30-subject SPI was scanned with a local-maximum search algorithm (Mintun *et al.,* 1989), to determine the locations of the M1-mouth areas (left and right) in the image with the highest possible signal to noise (i.e., the thirty-subject SPI). In this 30-subject image, several functional regions comprising the speech-motor system were readily identified, including: the left and right M1-mouth representations (BA4); supplementary motor area (medial BA6); the left ventral premotor region (BA6/44); and the left anterior insula (Table 3). The two M1-mouth locations (Table 3) were used to limit the search domain within the thirty, single-subject SPIs. Potential left and right M1-mouth loci were automatically detected as the most intense (highest positive *z* score) local maximum within a 3-cm radius of the grand-average M1-mouth locus. The large detection radius avoided artificially limiting the variance observed among loci. In 19 instances (10 left, 9 right), the most intense response within the search bound was not appropriate in location for M1-mouth. For example, the supplementary motor area was captured by the search algorithm in 1 case. Ventral premotor cortex (in humans, "Broca's area") was captured by the search algorithm in 14 cases. Superior temporal (in humans, "Wernicke's area") was captured in two cases and superior pre-motor was captured in two cases. In 11 instances (8 left; 3 right), the next most intense response was located appropriately for M1-mouth and was used for subsequent analysis. In 8 instances (2 left; 6 right), no M1-mouth response could be identified.

**TABLE 3**

Frontal-Lobe Speech-Motor Activations
(Group-Mean Image)

| Region | BA | X | Y | Z | *z* Score |
|---|---|---|---|---|---|
| M1-mouth (left) | 4 | −46 | −8 | 40 | 3.8 |
| M1-mouth (right) | 4 | 52 | −8 | 38 | 3.5 |
| SMA (bilat) | 6 | 0 | 4 | 53 | 3.7 |
| Ventral premotor (left) | 44 | −54 | −6 | 22 | 2.4 |
| Anterior Insula (left) | na | −30 | 2 | 10 | 2.0 |

*Note.* The coordinates of the speech related, motor-area activations derived from the group-mean image pooling 30 subjects from three 10-subject studies are reported. Ventral premotor is "Broca's area."

*Statistical analysis.* Loci resulting from the above-described image acquisition, pooling and searching stages were analyzed to determine: (1) whether the three Cohorts (used for original-data metanalysis) differed in the mean location or variability of M1-mouth; (2) whether the spatial distributions of the 30-subject sample differed significantly from Gaussian; (3) and, whether the literature-derived FVM model for M1-mouth correctly predicted the mean location, the location variability, and the location-probability profiles for the 30-subject original-data metanalysis. Finding intercohort equivalence, a normal distribution, and good agreement between literature and original-data metanalysis, a combined model of M1-mouth was generated, using all available data.

**TABLE 4**

Cohort Equivalence

| | Left | | | Right | | |
|---|---|---|---|---|---|---|
| Axis | C1 | C2 | C3 | C1 | C2 | C3 |
| X | −47 ± 4 | −44 ± 4 | −44 ± 5 | 50 ± 3 | 51 ± 3 | 48 ± 4 |
| Y | −10 ± 6 | −10 ± 7 | −10 ± 6 | −10 ± 5 | −7 ± 7 | −5 ± 6 |
| Z | 36 ± 5 | 38 ± 6 | 40 ± 4 | 36 ± 3 | 35 ± 7 | 39 ± 4 |

*Note.* Averages and standard deviations calculated per Cohort are presented for the left and right M1-mouth regions. The three Cohorts were effectively identical in the distribution of per-subject response loci (ANOVA, $F < 2.6$, $P > 0.1$). Based on this equivalence, data were pooled for assessment of image averaging, spatial distribution, and goodness-of-fit to model.

*Intercohort equivalence.* The equivalence of the mean location for M1-mouth among the three Cohorts (C1, C2, C3) was tested with an single-factor ANOVA. The homogeneity of variance across Cohorts was tested using the Bartlett test (Zar, 1996). Finding no differences, the Cohorts were pooled for all subsequent analyses (Table 4, below).

*Normality.* The cardinal assumption of functional volumes modeling is that response locations (within a laboratory) form a Gaussian distribution along each spatial axis. For graphical assessment of the normality of the per-subject location-distributions, responses were plotted by axis (x, y, z) and by hemisphere (Fig. 1, below), being compared to a Gaussian distribution with the same mean and standard deviation (Fig. 1). In addition, a pooled histogram was created by normalization of each of the six, individual-axis histograms to a zero-mean and unit-standard-deviation histogram (Fig. 2, below). All seven distributions (six per-axis and one pooled) were tested for normality by computing skew (gamma-one statistic) and kurtosis (gamma-two statistic) and applying the D'Angostino–Pearson $K^2$ test for normality (Zar, 1996).

*Fit of data to model.* The hypothesis that a model of the M1-mouth spatial distribution derived from the group-mean SPI literature would predict the location-probability profiles derived from individual subjects was tested. Spatial distributions were assessed graphically by entering individual response loci into the BrainMap database (Fox and Lancaster, 1996) and plotting them relative to the FVM-predicted bounds (Fig. 3, below). As a descriptive statistic, the percentage of responses lying within the model bounds, predicting the 50th, 68th, and 95th percentiles was determined (Table 7, below). Goodness of fit between the FVM profiles and the single-subject profiles were tested with a group *t* test.

*Consensus model.* In view of the agreement between the spatial probability profiles modeled from the literature and computed from original data, a consensus model was created which combined all available data. This was done by: (1) recomputing intersubject variability (Table 1) to include variability among the present thirty, single-subject data sets as two regions (left and right M1-mouth); (2) recomputing the FVM model of M1-mouth, including the M1-mouth coordinates from the present thirty-subject, group-mean image. The consensus model was computed both as single-axis profiles (Table 6, below) and as 3-D ellipsoids, for illustration purposes (Fig. 4b, below).

## RESULTS

*Detection frequency.* Detection frequency was high. A left, M1-mouth locus was detected in 28 of 30 (93%) persons. A right M1-mouth locus was detected in 24 of 30 (80%) persons.

*Intergroup equivalence.* M1-mouth responses were quite similar among the three Cohorts in both mean location and in variance about the mean (Table 4). While minor differences in mean location were observed, they did not approach statistical significance (ANOVA: $F$, 2.6; $P > 0.1$). Variability about the means was also homogenous across Cohorts, with standard deviations ranging from 3 to 7 mm (Table 4). Standard deviations did not differ among Cohorts (Bartlett Test, $P > 0.88$). Based upon this observed equivalence among the three groups in mean and variability about the mean, data were pooled across Cohorts for assessing the normality of the distributions' goodness-of-fit to the FVM model and the creation of a conjoined model.

*Profile normality.* The M1-mouth location-distribution profiles observed from these per-subject data appeared normal (i.e., Gaussian), within the limits of sample size (Fig. 1). This observation was statistically tested by computing the skew and kurtosis of the six profiles (three axes by two hemispheres). All values were near zero, as expected for a Gaussian distribution (Table 5). None differed significantly from zero (gamma-one and gamma-two statistics; Zar, 1996). In addition, the $K^2$ D'Agostino–Pearson statistic was not significant for any axes in either hemisphere ($P > 0.5$; Table 6). To further test this observation, the 156 per-subject observations (28 left hemisphere by 3 axes; 24 right hemisphere by 3 axes) were normalized to a zero mean and unit standard deviation, pooled, and compared to a unit normal distribution (Fig. 2). The gamma and $K^2$ D'Agostino–Pearson statistics for the pooled distribution (156 observations) were not significantly different from Gaussian ($P > 0.6$). These observations support the FVM modeling assumption that location-distribution profiles are normal.

*Fit of original-data metanalysis to literature-derived model.* The FVM-modeled mean location for left M1-mouth was: −47, −13, 36 (x, y, z). The FVM-modeled mean location for right M1-mouth was: 47, −9, 35 (x, y,

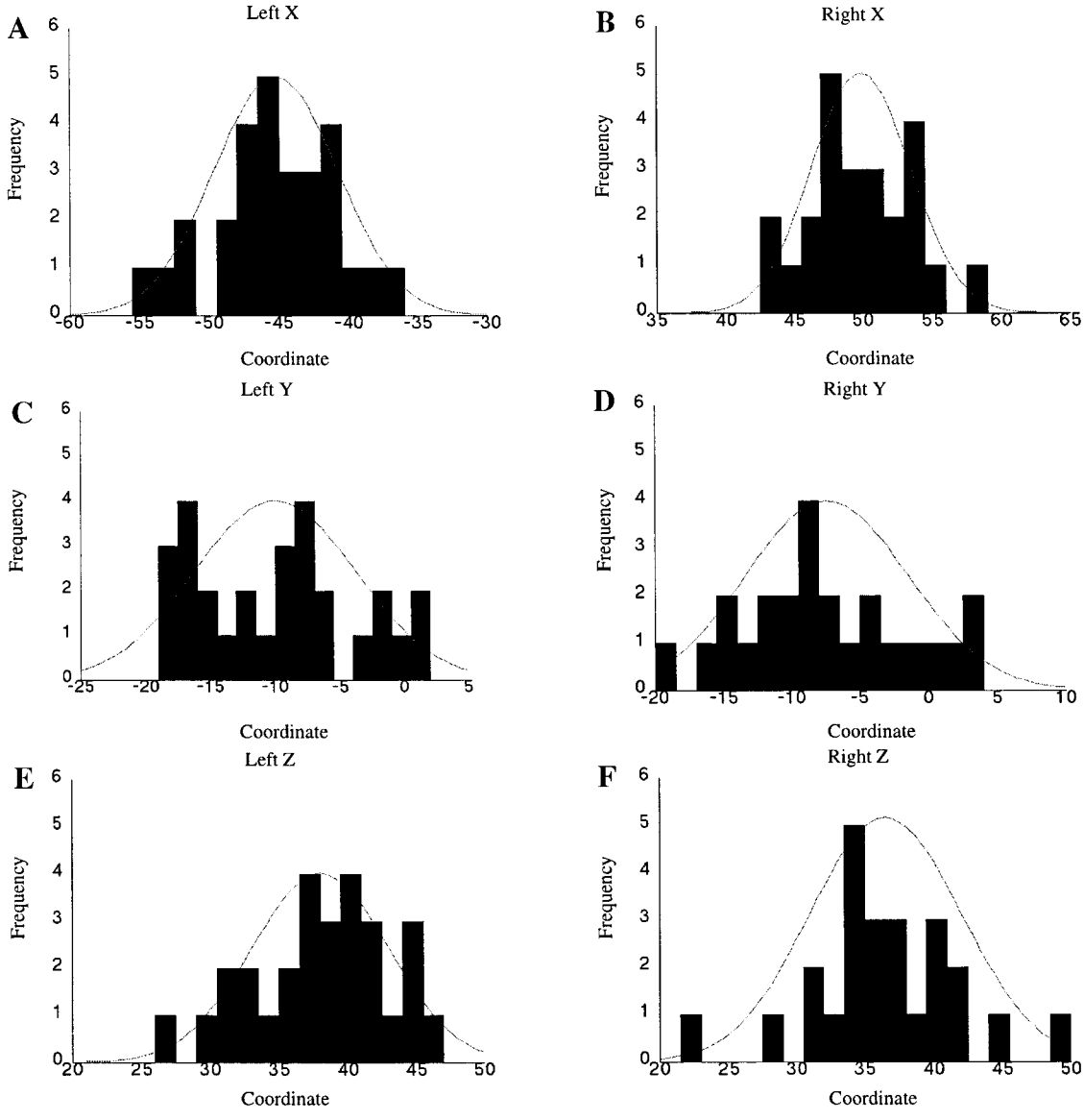


**FIG. 1.** Normality of M1-mouth location distributions by hemisphere and axis. Location-distribution profiles derived from 30 individual subjects for the left M1-mouth region (A = x; C = y; E = z), the right M1-mouth region (B = x; D = y; F = z) are shown. The spatial distributions of the M1-mouth responses were not significantly different from Gaussian.

z). Each of these values was within 5 mm of the mean of the 30, single-subject images. No significant differences were found for any axis (unpaired *t* test, uncorrected for multiple comparisons). Variability was quite close to that predicted from literature metanalysis (compare Table 5 with Table 1). Variability did not differ among axes or hemispheres (Bartlett test, $P > 0.8$). Observed location-distribution profiles were in good agreement with predicted (Table 7; Fig. 3). None differed significantly from predicted (*t* test).

*Consensus model.* As the literature-derived and original-data derived spatial probability distributions were in good agreement, a consensus model was computed that combined all available data (Table 6 and Fig. 4b, below). The consensus model represents the best available estimate of the 3-D spatial probability profiles for M1-mouth.

## DISCUSSION

The M1-mouth mean location, location variability and spatial-probability contours derived from metanalysis of the group-mean literature were in good agreement with values determined from per-subject mapping in thirty normal volunteers. Original-data and intersubject variability values were small and consistent between hemispheres and among coordinates axes, as predicted. These results indicate that stan-

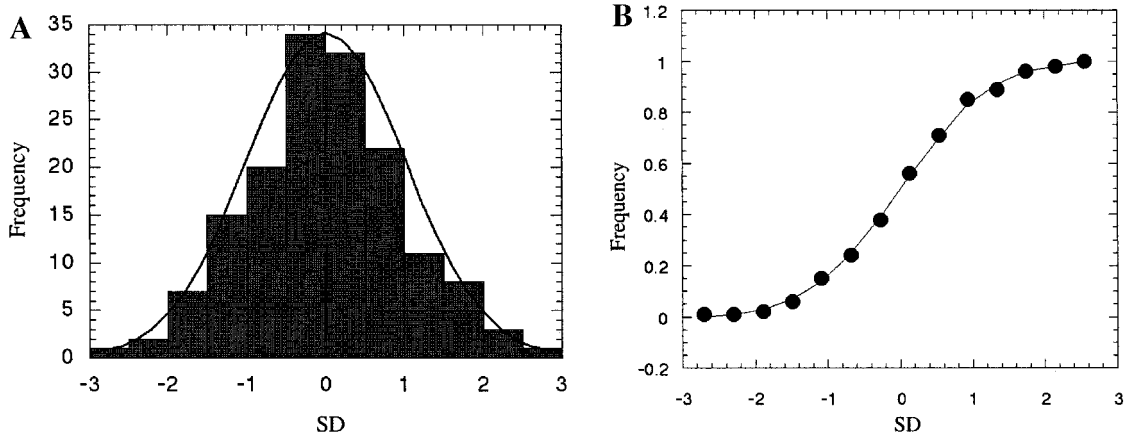


**FIG. 2.** Normality of the pooled M1-mouth location distribution. A pooled location-distribution profile (combining coordinates for both hemisphere and all three axes) was computed by normalizing the individual location-distribution profiles. The cumulative profile is compared to the unit normal distribution with the same mean and variance (solid line) both as a frequency histogram (A) and as a cumulative frequency histogram (B). The cumulative location distribution profile did not differ significantly from the unit normal distribution (the gamma and $K^2$ D'Agostino-Pearson statistic, $P > 0.6$; Zar, 1996).

dardized coordinates provide an effective alternative to surface anatomy for describing the location of cortical functional areas and for predicting intersubject variability. Within this spatial construct, present data provide the most rigorous description to date of the location and location variability of the M1-mouth representation. Finally, present results indicate that spatial probability modeling, in general, has considerable predictive power and that metanalytic modeling of group-mean data (i.e., FVM), in particular, has predictive power comparable to that of individual-subject data for constructing spatial probability profiles.

*Mean location.* The mean locations of the M1-mouth representations (left and right) independently modeled from a metanalysis of the grand-mean, neuroimaging literature (71 subjects) and from an original-data metanalysis of data from thirty individual subjects were in good agreement with one another (Figs. 4a and 4b). These models were also in good agreement with prior descriptions of the location and location variability of this functional region (Figs. 4c–4e), as follows. Penfield reported the location and somatotopic organization of M1-mouth cortex in the now-classic, "homonculus" diagram, which subjectively synthesized intraoperative cortical stimulation results from hundreds of patients (Penfield and Rasmussen, 1950). Note that while responses in areas other than hand, face and foot are difficult to elicit, Penfield's diagram interpolates between observations to give a continuous representation of the body, the continuity of which has not been confirmed. Talairach *et al.* (1967) reported per-subject, 3-D coordinates of brain locations at which intraoperative cortical electrical stimulation elicited movements of face, hand, or foot (Fig. 4c), providing the first quantitative descriptions of the motor cortex homonculus and of the M1-mouth location, in particular. Fox *et al.* (1987a) reported per-subject, 3-D coordinates of brain locations activated during cutaneous stimulation of face, hand, or foot, based on PET blood-flow imaging, using Talairach's standardized space (Fig. 4d). Grafton *et al.* (1991) reported per-subject locations (in polar coordinates referenced to a coronal plane) activated by voluntary movements of mouth, hand, or leg, also using PET blood-flow imaging (Fig. 4e). Despite the differences in mapping methodology and reporting convention, the agreement among these several studies is remarkable (compare Figs. 4a–4e). Similarly, the agreement among the group-mean reports of the M1-mouth location (used as for input to the model) is also noteworthy (Table 2).

The designation of the reported locations as M1-mouth merits some discussion. Speech was the motor component of the task used in all five studies providing input data for the metanalytic modeling (Table 2) and in all three 10-subject cohorts used for per-subject localization of M1-mouth. Although principally a motor task, speech necessarily involves proprioceptive feedback, thus simultaneously activating primary sensory cortex (BA 3,1,2) as well as primary motor cortex (BA 4). When M1 and S1 response foci lie closer to one another than the spatial resolution of the imaging system, they will merge into a single focus whose location is the center-of-mass of the merged M1-S1 response. Response merging, although common, is not universal; clearly independent M1 and S1 responses were observed in about a half of the 30, individually mapped subjects. From these subjects, it was apparent that M1 and S1 responses may be offset in depth (one lying nearer the gyral convexity, the other lying nearer the sulcal pit) or in position along the central sulcul (one being more dorsal, the other more ventral). Nevertheless, the response locations reported are likely some-

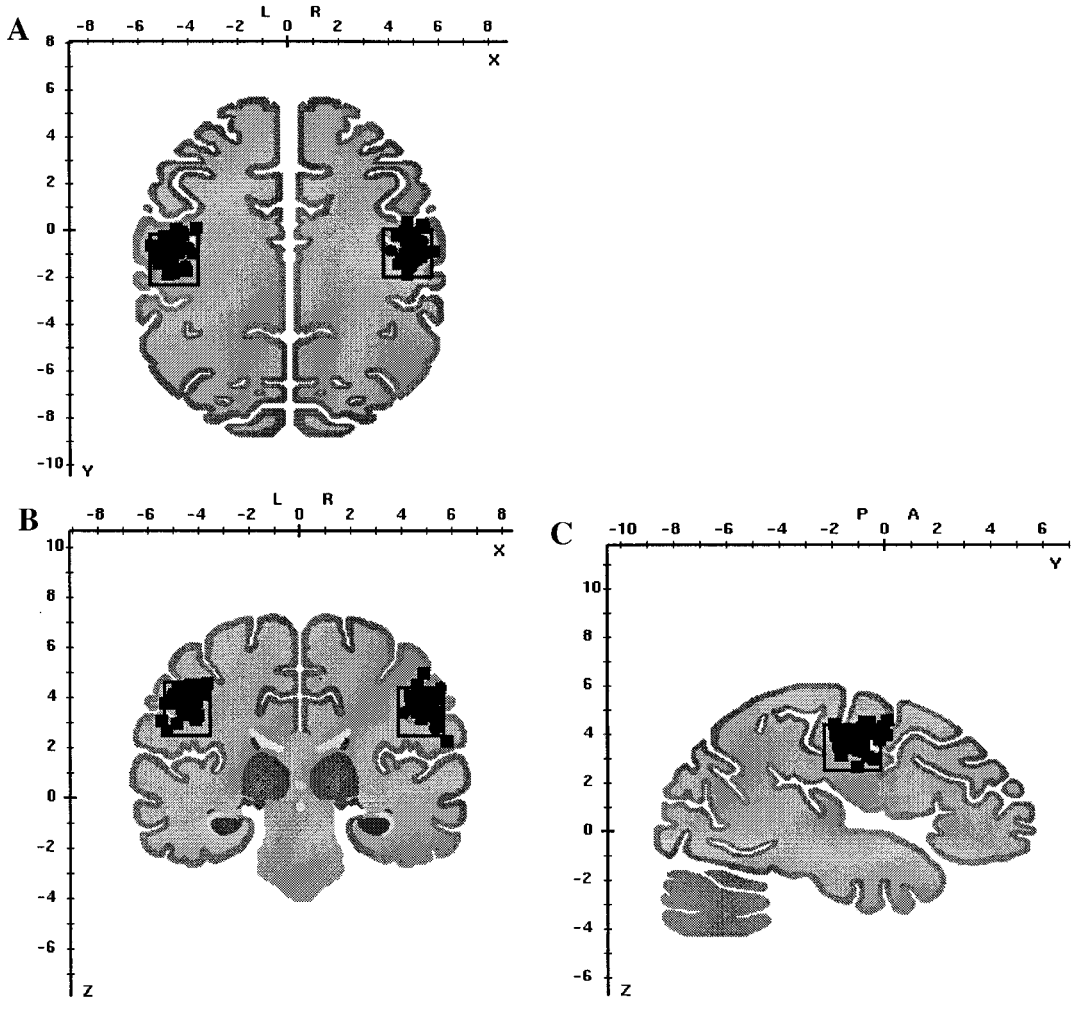


**FIG. 3.** Fit of original-data metanalysis to literature-derived model. The location distribution of the M1-mouth responses (28 left; 24 right) from 30 subjects are illustrated relative to the prediction of the literature-derived FVM model. The rectangle illustrates the predicted 95% confidence bounds. Locations are, in millimeters referable to Talairach (1988), plotted in the Search and View interface of the BrainMap database (Fox and Lancaster, 1996) in axial $z = 35$ (A), coronal $y = -24$ (B), and sagittal $x = -43$ (C) views.

what posterior to those observed with a pure motor task (e.g., during blocking of somatosensory feedback) or with a higher resolution imaging modality, such as functional MRI. This effect is likely not very large, as S1 activations during lip vibration lay, on average, 12 mm posterior to the M1 locations reported here (Fox *et al.*, 1987), indicating that present results were minimally influenced by somatosensory activations. It should also be noted that speech production requires movements of the larynx and diaphragm as well as of the mouth (i.e., the lips, tongue, and oropharynx). Thus, the response locations have some contributions from nonoral structures. The cortical representation of larynx and diaphragm, however, are not likely to be large relative to other oral structures, making their weighting of the reported response locations rather minor.

**TABLE 5**

Normality of Single-Subject Location-Distribution Profiles

| | Left | | Right | |
|---|---|---|---|---|
| Axis | $\gamma 1$ | $\gamma 2$ | $\gamma 1$ | $\gamma 2$ |
| X | −0.1 | +0.3 | +0.3 | −0.2 |
| Y | +0.3 | −1.0 | +0.2 | −0.6 |
| Z | −0.5 | −0.2 | 0.0 | +1.4 |

*Note.* The location-distribution profiles derived from the thirty individuals were tested for normality. Skew ($\gamma 1$ statistic) and kurtosis ($\gamma 2$ statistic) were near zero, the expected values for a normal distribution, for both hemispheres and all three axes (x, y, z). No value differed significantly from normal.

*Intersubject variability.* The average of the standard deviations (pooling x, y, and z) determined from the original-data-metanalysis (Table 6) component of the present study agreed very closely with the average

**TABLE 6**

Fit of Original-Data Metanalysis to Literature-Derived Model (FVM): Mean and Variance

| Side | | *n* | X | Y | Z |
|---|---|---|---|---|---|
| Left | Modeled | 71 | −47 ± 5.2 | −13 ± 5.6 | 36 ± 5.5 |
| | Observed | 28 | −45 ± 4.4 | −10 ± 6.2 | 38 ± 5.0 |
| | Consensus | 99 | −46 ± 5.2 | −11 ± 5.6 | 35 ± 5.5 |
| Right | Modeled | 71 | 47 ± 5.3 | −9 ± 5.6 | 35 ± 5.5 |
| | Observed | 24 | 50 ± 3.6 | −7 ± 6.0 | 36 ± 5.5 |
| | Consensus | 99 | 48 ± 5.2 | −9 ± 5.6 | 35 ± 5.5 |

*Note.* The mean ± one standard deviation of the thirty-subject, original-data metanalysis (observed) are compared with those modeled by FVM from the two literature metanalyses (modeled). The agreement is very close. The mean (two tailed *t* test, $P > 0.5$) did not differ between modeled and observed. A consensus model was computed by adding the 30-subject data to computations of intersubject variability (Table 1) and the M1-mouth mean location (Table 2).

of literature-reported values (Table 1), being 5.3 mm and 5.6 mm (SD), respectively. While the variability among the six, single-subject, standard deviations (two hemispheres by three axes) was small (range of 4 to 6 mm), the variability among standard deviations reported in the literature is quite large, ranging from 2 to 13 mm (Table 1). Even within a single study, estimates of function-location standard deviation can range from 3 mm to 13 mm (Table 1). In large measure, the consistency of the variability estimates of the present study can be attributed to sample size. The present study, to our knowledge, is the largest (30 persons; 52 M1-mouth values), within-laboratory report of the intersubject variability of the spatial coordinates of any functional brain area. An additional factor allowing the present study to provide better and more consistent estimates of location variability than prior studies was the very high signal-to-noise ratio of the activation images. Mintun *et al.* (1989) demonstrated that the precision of the estimation of functional location is strongly dependent upon the signal-to-noise ratio of the subtraction image. While prior PET studies reporting location variability have typically relied on single trial data, the present study used two or three trials on each task, thus increasing response-localization precision and reliability.

The present study determined the location and location variability of only two brain functional areas: the left and right M1 mouth representations. Thus, present data do not directly address whether location variability is similar across different functional areas. Functional volumes modeling, however, assumes that the intersubject component of location variability of brain functional areas is similar for all functional areas, in that it uses a single variance parameter derived from location-variability values reported for a variety of brain areas. The goodness of the predictive capability of FVM will depend upon the closeness of the variability of the modeled area(s) to the average variability value (used for modeling). Areas with greater or less variability than average will be less well modeled. The most readily modeled circumstance would be for all functional brain areas to have similar location variability. This is suggested by the collective experience of studies of reporting individual variability (Table 1) and by studies which simultaneously assessed variability in several functional areas, including Fox and Pardo (1991; Table 1), Hasnain *et al.* (1998; Table 1) and Hunton *et al.* (1996; Table 1). These studies not withstanding, the assumption of homogenous variance needs further validation. The most economical means to this end is to perform additional original-data metanalyses for a variety of brain functional areas, preferably in the context of creating and validating additional FVM, location-probability profiles.

The spatial probability modeling performed here (FVM), assumed that intersubject location variability formed a Gaussian distribution. Data from 30 individual subjects tentatively confirmed this assumption (Figs. 2 and 3; Table 7). Normality of the spatial distributions of other functional areas has also been suggested by Fox *et al.*, (1997), Hunton *et al.* (1996), Hasnain *et al.* (1998).

*Spatial probability profiles.* In the present report the location of M1-mouth is reported in terms of a spatial probability profiles, which describies the cumulative likelihood of an event over a spatial domain. Talairach introduced the use of spatial probability models to human brain mapping, using this format to describe and display intersubject variability in brain structure and function (Talairach *et al.*, 1967). Following the introduction of Talairach coordinates to human brain mapping, several investigators have reported intersubject variability of brain functional areas (Table 1), but without modeling spatial probability profiles. Over the past several years, however, the use of spatial probability profiles to quantify and display intersubject variability has seen considerable interest. In particular, Toga, Thompson, and colleagues have pioneered the use of 3-D spatial probability models to describe the distribution of features of the cortical surface (Thompson and Toga, 1996a, b; Thompson *et al.*, 1997). Fox and colleagues have applied a form of spatial probability modeling (termed "penetrance imaging") to several brain areas activated during speech tasks (Fox *et al.*, 1996). The present application of functional volumes modeling extends the use of spatial probability models for the quantitative description of brain functional organization, increasing the mathematical formality of the computation and validating the practice of modeling spatial probabilities from group mean data.

In the present paper, the validations were limited to one-dimensional probabilities (probability profiles) in each cardinal axis. Fully three-dimensional probability

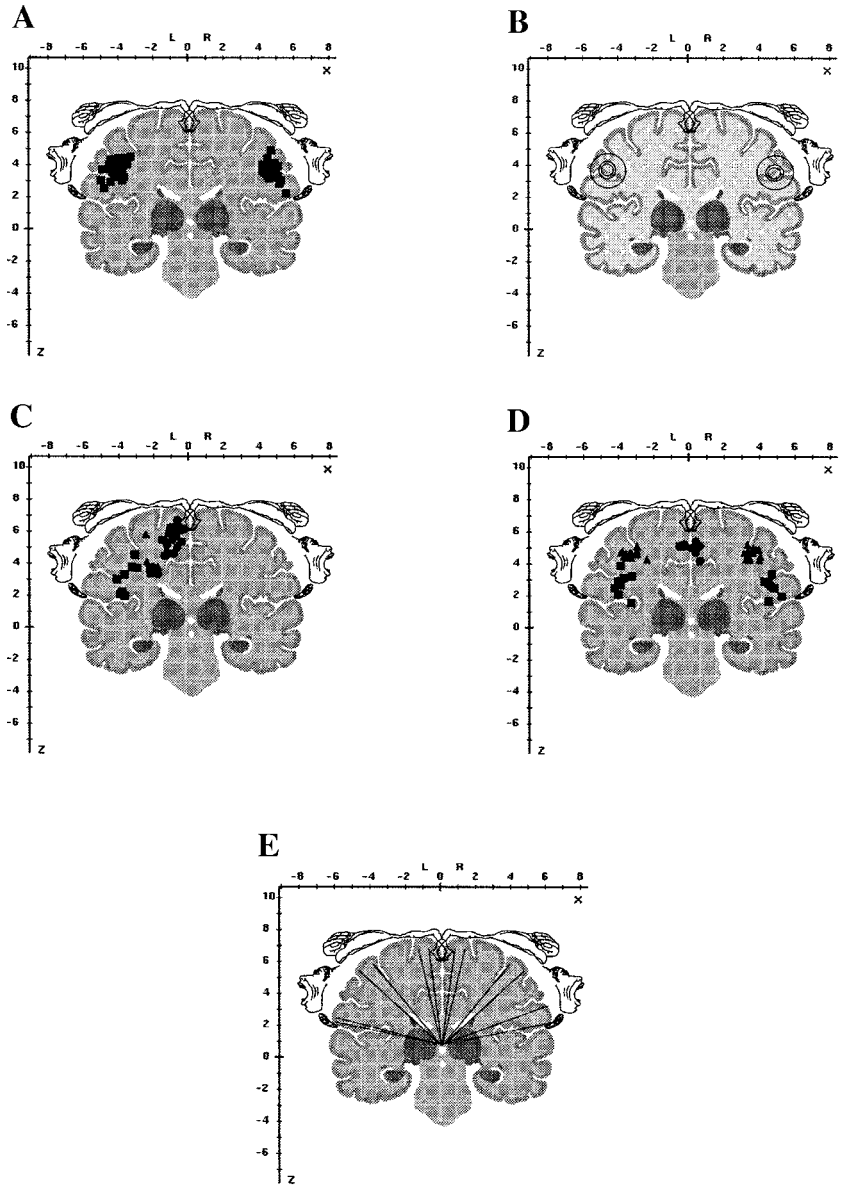


**FIG. 4.** Comparison of homunculi. The classical homunculus of Penfield is compared to quantitatively described (i.e., coordinate referenced) studies, both invasive and noninvasive. (A) Present data for the M1-mouth location from 30 normal subjects. (B) The 50, 68, and 95% confidence bounds of the consensus model, computed as 3-D elipsoids (rather than 1-D profiles) (Table 6). (C) Locations for M1 face/tongue (square), hand (triangle), and foot (circle) derived from intraoperative electrical stimulations (Talairach *et al.*, 1967). (D) Locations for S1 mouth (square), hand (triangle), and foot (circle) derived from PET imaging during vibratory stimulation (Fox *et al.*, 1987). (E) Sectors representing polar-coordinate bounds for M1 mouth, hand, and leg reported by Grafton *et al.* (1991). All images (A–E) are plotted in the Search and View Interface of the BrainMap database at slice −24 mm in the y plane.

volumes were created for illustration purposes, but have not been validated. A probability volume is clearly preferable to a set of profiles, providing a more precise representation of the spatial distribution. Validation of probability volumes will be undertaken in subsequent phases of this work.

*Surface landmarks.* In the present study, the locations of functional areas are described relative to a standardized space with no explicit reference to surface anatomical features, such as sucli and gyri. The use of M1-mouth as the "test case" for spatial probability modeling of a brain functional area was motivated, in part, by Grafton's observation that the M1-mouth area "was identified by no sulcus or other surface landmark." Despite the lack of a reliable surface-anatomical reference point, the M1-mouth location was reliably located for individual subjects by a spatial probability model computed from group-mean data. Moreover, the observed intersubject variability of the M1-mouth location was quite similar to the average

**TABLE 7**

Fit of Original-Data Metanalysis to Literature-Derived Model (FVM): Location-Distribution Profiles

| Side | *n* | Axis | 50% | 68% | 95% |
|---|---|---|---|---|---|
| Left | 28 | X | 57.1 | 78.6 | 100.0 |
| | | Y | 39.3 | 57.1 | 89.3 |
| | | Z | 28.6 | 46.4 | 85.7 |
| | | Mean | 41.7 | 60.7 | 91.7 |
| Right | 24 | X | 62.5 | 91.7 | 100.0 |
| | | Y | 41.7 | 58.3 | 91.7 |
| | | Z | 37.5 | 50.0 | 91.7 |
| | | Mean | 47.2 | 66.7 | 94.4 |

*Note.* The percentage per-subject observations falling within the location-distribution profiles predicted by FVM modeling of M1-mouth from literature metanalysis are shown. "Side" indicates the cerebral hemisphere. The "*n*" column indicates the number of subjects (of 30) in which an M1-mouth response was detected. "Axis" indicates the cardinal axes of the standardized coordinate space. The 50, 68, and 95% columns indicate the percentage of the per-subject observations falling within the bounds predicted by FVM to contain 50, 68, and 95% of the observations, respectively.

of that reported for other brain areas (Table 1). In view of the known complexity and intersubject variability of the gyrification of the posterior, inferior frontal lobe (Ono, 1990; Garey, 1994), this supports suggestions that gyral complexity and intersubject variability in gyral anatomy are not indicative of the intersubject variability in local functional anatomy (Fox and Pardo, 1991). This further suggests that the impression that language related brain areas are particularly variable in location (Ojemann *et al.*, 1989) may reflect the unreliability of surface features as an anatomical reference frame, rather than true variability in the locations of functional areas.

*Influence of spatial normalization algorithms.* All image data used in this report, both literature-derived and in-house, were spatially normalized using global, linear spatial normalization algorithms (e.g., Lancaster *et al.*, 1995, 1999), rather than regional, nonlinear (e.g., Christensen *et al.*, 1994; Schormann *et al.*, 1998; Collins *et al.*, 1999; Kochunov *et al.*, 1999). That is, spatial transformations were limited to translations, rotations and scales along each coordinate axis with no regionally specific deformations. Thus, the spatial probability profiles reported here describe intersubject variability, assuming prior global spatial normalization. Although generally similar in their methodologies, global spatial normalization algorithms differ among laboratories. Interlaboratory differences in spatial normalization methodology could influence present estimates of variability in two ways. First, differences among laboratories in reported estimates of intersubject variability (Table 1) likely reflect differences in algorithm performance as well as true differences between brain areas and subject samples. Second, a laboratory-specific algorithmic bias would contribute to interlaboratory differences in the reported mean locations of M1-mouth (Table 2). Such errors would influence the estimated mean location of the M1-mouth FVM model in direct proportion to the number of subjects in each laboratory's group. Such errors, however, would not influence our estimate of intersubject variability, as this was derived entirely from the data in Table 1.

Regional spatial normalization algorithms were not employed for several reasons. Regional spatial normalization algorithms (Christensen *et al.*, 1994; Schormann *et al.*, 1998; Collins *et al.*, 1999; Kochunov *et al.*, 1999) are at an early stage of development. To our knowledge, no functional brain mapping papers—and certainly none of the papers reporting the location of M1-mouth—have used algorithms of this type. Data transformed with this degree of anatomical precision, then, are not available. As a consequence, the impact that nonlinear spatial normalization will have on functional variability is unknown. Although these algorithms can remove nearly all of the anatomical variability between subjects, it remains conjectural whether or not this will substantially decrease intersubject variability in functional-area locations and, if so, whether this improvement will be equal for all brain regions or only for regions near primary sulci. It is well known that the locations of many brain functional areas, including M1-mouth, are not reliably predicted by gross anatomy (i.e., surface features). Thus, using spatial normalization algorithms which mimimize differences in surface anatomy may or may not reduce functional variability below that achieved by global algorithms. Estimation of the intersubject functional-area variability following nonlinear anatomical matching, then, remains an objective for future work.

*Applications.* Several motivations for performing metanalysis of functional areas can be identified. First and foremost, metanalytic models serve as accurate, concise, intuitive formulations of accumulated knowledge, as is illustrated here. In addition, models can serve as tools for automated image analysis, image interpretation, and data retrieval. As an example of image interpretation, a location-probability model (either structural or functional) can be used to assign a most-likely name and an likelihood value to a feature within a brain image (e.g., an activated location). Structure–location names and probabilities are already being used for this purpose (Lancaster *et al.*, 1997). Functional spatial–probability contours could be used in a similar manner. Functional location–probability contours can be used as a regions-of-interest, to specify locations within an activation image hypothesized to be engaged by a task. By this model, analysis would ask whether or not the hypothesized areas (defined by location–probability boundaries) were acti-

vated under a specific set of conditions, thereby directly addressing the recurring criticism that voxel-based image analyses are intrinsically hypothesis generating rather than hypothesis testing (Worsley *et al.*, 1992; Friston *et al.*, 1991; Ford, 1986). This strategy would also increase statistical power, by reducing the analyzed volumes, thereby reducing the severity of the correction for multiple comparisons (Friston *et al.*, 1997). Precise description of location–probability distributions for the normal-subject population provides a powerful tool for identifying aberrant organizations, such as likely occur with developmental and acquired brain lesions. Spatial probability models can also be used to guide experimental or therapeutic interventions. For example, Paus and colleagues have used probabilistic estimates of mean location to guide delivery of transcranial magnetic stimulation (Paus *et al.*, 1997, 1998). Finally, retrieval of studies activating a specific brain location from a database, such as BrainMap (Fox and Lancaster, 1996), can be readily and powerfully performed by means of location–probability bounds.

## ACKNOWLEDGMENTS

This work was supported by NIH Grants MH/DA52176, DC03689, LM6858, and by grants from the EJLB Foundation and the Mind Science Foundation.

## REFERENCES

Andreasen, N. C., O'Leary, D. S., Cizadlo, T., Arndt, S., Rezai, K., Watkins, G. L., Ponto, L. L. B., and Hichwa, R. D. 1995. Remembering the Past: Two facets of eposidic memory explored with positron emission tomography. *Am. J. Psych.* **152:** 1576–1585.

Belliveau, J. W., Kennedy, D. N., Mckinstry, R. C., Buchbinder, B. R., Weisskoff, R. M., Cohen, M. S., Vevea, J. M., Brady, T. J., and Rosen, B. R. 1991. Functional mapping of the human visual cortex by magnetic resonance imaging. *Science* **254:** 716–719.

Bookheimer, S. Y., Zeffiro, T. A., Blaxton, T., Gaillard, W., and Theodore, W. 1995. Regional cerebral blood flow during object naming and word reading. *Hum. Brain Mapp.* **3:** 93–106.

Braun, A. R., Varga, M., Stager, S., Schulz, G., Selbie, S., Maisog, J. M., Carson, R. E., and Ludlow, C. L. 1997. Altered patterns of cerebral activity during speech and language production in developmental stuttering. *Brain* **120:** 761–784.

Christensen, G., Rabbitt, R., and Miller, M. 1994. 3-D brain mapping using a deformable neuranatomy. *Phys. Med. Biol.* **39:** 609–618.

Collins, D., Holmes, C., Peter, T., and Evans, A. 1999. ANIMAL: Automated Nonlinear Image Matching and Anatomical Labeling. In *Brain Warping* (A. Toga, Ed), pp. 133–142. Academic Press, San Diego.

Ford, I. 1986. Confounded correlations: Statistical limitations in the analysis of interregional relationships of cerebral metabolic activity. *J. Cereb. Blood Flow Metab.* **6:** 385–388.

Fox, P. T. 1995a. Broca's area: Motor encoding in somatic space. *Behav. Brain Sci.* **18**(2): 344–345.

Fox, P. T. 1995b. Spatial normalization: Origins, objectives, applications and alternatives. *Hum. Brain Mapp.* **3:** 161–164.

Fox, P. T., Burton, H., and Raichle, M. E. 1987a. Mapping human somatosensory cortex with positron emission tomography. *J. Neurosurg.* **67:** 34–43.

Fox, P. T., Fox, J. M., Raichle, M. E., and Burde, R. M. 1985a. The role of cerebral cortex in the generation of voluntary saccades: A positron emission tomographic study. *J. Neurophysiol.* **54:** 348–369.

Fox, P. T., Ingham, R. J., Ingham, J. C., Hirsch, T. B., Downs, J. H., Martin, C., Jerabek, P., Glass, T., and Lancaster, J. L. 1996. A PET study of the neural systems of stuttering. *Nature* **382:** 158–162.

Fox, P. T., and Lancaster, J. L. 1996. Un atlas du cerveau sur internet. *La Recherche* **289:** 49–51.

Fox, P. T., Lancaster, J. L., Parsons, L. M., Xiong, X. H., and Zamaripa, F. 1997. Functional volumes modeling: Theory and preliminary assessment. *Hum. Brain Mapp.* **5:** 306–311.

Fox, P. T., Miezin, F. M., Allman, J. M., Van Essen, D. C., and Raichle, M. E. 1987b. Retinotopic organiztion of human visual cortex mapped with positron-emission tomography. *J. Neurosci.* **7:** 911–922.

Fox, P. T., Mintun, M. A., Raichle, M. E., and Herscovitch, P. 1984. A noninvasive approach to quantitative functional brain mapping with $H_2^{15}O$ and positron emission tomography. *J. Cereb. Blood Flow Metab.* **4:** 329–333.

Fox, P. T., Mintun, M. A., Reiman, E. M., and Raichle, M. E. 1988. Enhanced detection of focal brain responses using intersubject averaging and distribution analysis of subtracted PET images. *J. Cereb. Blood Flow Metab.* **8:** 642–653.

Fox, P. T., and Mintun, M. A. 1989. Noninvasive functional brain mapping by change-distribution analysis of average PET images of $H_2^{15}O$ tissue activity. *J. Nucl. Med.* **30:** 141–149.

Fox, P. T., and Pardo, J. 1991. Does inter-subject variability in cortical functional organization increase with neural "distance" from the periphery? In *Exploring Brain Functional Anatomy with Positron Tomography*, pp. 125–144. Wiley, New York.

Fox, P. T., Parsons, L. M., and Lancaster, J. L. 1998. Beyond the single study: Function/location metanalysis in cognitive neuroimaging. *Curr. Opin. Neurobiol.* **8:** 178–187.

Fox, P. T., Perlmutter, J. S., and Raichle, M. E. 1985b. A stereotactic method of anatomical localization for positron emission tomography. *J. Comput. Assist. Tomogr.* **9:** 141–153.

Fox, P. T., Raichle, M. E., and Thach, W. T. 1985c. Functional mapping of the human cerebellum with positron emission tomography. *Proc. Natl. Acad. Sci. USA* **82:** 1–5.

Friston, K. J., Frith, C. D., Liddle, P. F., and Frackowiak, R. S. J. 1991. Comparing functional (PET) images: The assessment of significant change. *J. Cereb. Blood Flow Metab.* **11:** 690–699.

Friston, K. J. 1997. Testing for anatomically specified regional effects. *Hum. Brain Mapp.* **5:** 133–136.

Garey, L. J. 1994. *Brodmann's Localization in the Cerebral Cortex.* Smith Gordon, London.

Goldring, S. 1978. A method for surgical management of focal epilepsy expecially as it relates to children. *J. Neurosurg.* **49:** 344–356.

Grafton, S. T., Woods, R. P., and Mazziotta, J. C. 1993. Within-arm somatotopy in human motor areas determined by positron emission tomography imaging of cerebral blood flow. *Exp. Brain Res.* **95:** 172–176.

Grafton, S. T., Woods, R. P., Mazziotta, J. C., and Phelps, M. E. 1991. Somatotopic mapping of the primary motor cortex in humans: Activation studies with cerebral blood flow and positron emission tomography. *J. Neurophysiol.* **66:** 735–743.

Hasnain, M. K., Fox, P. T., and Woldorff, M. G. 1998. Intersubject variability of functional areas in the human visual cortex. *Hum. Brain Mapp.* **6:** 301–315.

Herscovitch, P., Markham, J., and Raichle, M. E. 1983. Brain blood flow measured with intravenous $H_2^{15}O$. I. Theory and error analysis. *J. Nucl. Med.* **24:** 782–789.

Hunton, D. L., Miezin, F. M., Buckner, R. L., van Mier, H. I., Raichle, M. E., and Petersen, S. E. 1996. An assessment of functional-anatomical variability in neuroimaging studies. *Hum. Brain Mapp.* **4:** 122–139.

Kochunov, P., Lancaster, J., and Fox, P. 1999. Accurate high-speed spatial normalization using an octree method. *NeuroImage* **10:** 724–737.

Lancaster, J. L., Glass, T. G., Lankipalli, B. R., Downs, H., Mayberg, H., and Fox, P. T. 1995. A modality-independent approach to spatial normalization of tomographic images of the human brain. *Hum. Brain Mapp.* **3:** 209–223.

Lancaster, J. L., Rainey, L. H., Summerlin, J. L., Freitas, C. S., Fox, P. T., Evans, A. E., Toga, A. W., and Mazziotta, J. C. 1997. Automated labeling of the human brain: A preliminary report on the development and evaluation of a forward-transform method. *Hum. Brain Mapp.* **5:** 238–242.

Lancaster, J., Fox, P., Downs, H., Hander, T., Mallah, M., and Zamarripa, F. 1999. Global spatial normalization of the human brain using convex hulls. *J. Nucl. Med.* **40:** 942–955.

Mintun, M. A., Fox, P. T., and Raichle, M. E. 1989. A highly accurate method of localizing regions of neuronal activation in the human brain with positron emission tomography. *J. Cereb. Blood Flow Metab.* **9:** 96–103.

Murphy, K., Corfield, D. R., Guz, A., Fink, G. R., Wise, R., Harrison, J., and Adams, L. 1997. Cerebral areas associted with motor control of speech in humans. *J. Appl. Physiol.* **83:** 1438–1447.

Ojemann, G., Ojemann, J., Lettich, E., and Berger, M. 1989. Cortical language localization in the left, dominant hemisphere. *J. Neurosurg.* **71:** 316–326.

Ono, M., Kubik, S., and Abernathey, S. A. 1990. *Atlas of the Cerebral Sulci.* Theime Medical, New York, NY.

Parsons, L. M., and Fox, P. T. 1998. The neural basis of implicit movements used in recognizing hand shape. *Cogn. Neuropsychol.* **15:** 583–615.

Paus, T., Petrides, M., Evans, A. C., and Meyer, E. 1993. Role of the human anterior cingulate ortex in the control of oculomotor, manual, and speech responses: A positron emission tomography study. *J. Neurophysiol.* **70:** 453–469.

Paus, T., Jech, R., Thompson, C. J., Comeau, R., Peters, T., and Evans, A. 1997. Transcranial magnetic stimulation during positron emission tomography: A new method for studying connectivity of the human cerebral cortex. *J. Neurosci.* **17:** 3178–3184.

Paus, T., Jech, R., Thompson, C. J., Comeau, R., Peters, T., and Evans, A. 1998. Dose-dependent reduction of cerebral blood flow during rapid-rate transcranial magnetic stimulation of human sensorimotor cortex. *J. Neurophysiol.* **79:** 1102–1107.

Penfield, W., and Rasmussen, T. 1950. *The Cerebral Cortex Of Man.* Macmillian, New York.

Petersen, S. E., Fox, P. T., Posner, M. I., Mintun, M., and Raichle, M. E. 1988. Positron emission tomographic studies of the cortical anatomy of single word processing. *Nature* **362:** 342–345.

Petrides, M., Alivisatos, B., Meyer, E., and Evans, A. C. 1993. Functional activation of the human frontal cortex during the performance of verbal working memory tasks. *Proc. Natl. Acad. Sci. USA* **90:** 878–882.

Raichle, M. E., Martin, W. R. W., Herscovitch, P., Mintun, M., and Markham, J. 1983. Brain blood flow measured with $H_2^{15}O$. II. Implementationand validation. *J. Nucl. Med.* **24:** 190–198.

Ramsey, N. F., Kirkby, B. S., Van Gelderen, P., Berman, K. F., Duyn, J. H., Frank, J. A., Mattay, V. S., Van Horn, J. D., Esposito, G., Moonen, C. T. W., and Weinberger, D. R. 1996. Functional mapping of human sensorimotor cortex with 3D BOLD correlates highly with $H_2^{15}O$ PET rCBF. *J. Cereb. Blood Flow Metab.* **16:** 755–764.

Schneider, W., Casey, B. J., and Noll, D. 1994. Functional MRI mapping of stimulus rate effects across visual processing stages. *Hum. Brain Mapp.* **1:** 117–133.

Schormann, T., and Zilles., K. 1998. Three-dimensional linear and nonlinear transformations: An integration of light microscopical and MRI data. *Hum. Brain Mapp.* **6:** 339–347.

Sobel, D. F., Gallen, C. C., and Schwartz, B. J., *et al.* 1993. Locating the central sulcus: Comparison of MR anatomical and magnetoencephalographic functional methods. *Am. J. Neurol. Radiol.* **14:** 915–925.

Strother, S. C., Lange, N., Anderson, J. R., Schaper, K. A., Rehm, K., Hansen, L. K., and Rottenberg, D. A. 1997. Activation pattern reproducibility: Measuring the effects of group size and data analysis models. *Hum. Brain Mapp.* **5:** 312–316.

Talairach, J., Szikla, G., Tournoux, P., Prossalentis, A., Borda-Ferrer, M., Covello, L., Iacob, M., and Mempel, E. 1967. *Atlas D'Anatomie Stereotaxique du Telencephale.* Masson, Paris.

Talairach, J., and Toumoux, P. 1988. *Coplanar Stereotaxic Atlas of the Human Brain.* Thieme, New York.

Thompson, P., and Toga, A. 1996. A Surface-based technique for warping three-dimensional images of the brain. *IEEE Tans. Med. Imag.* **15:** 402–408.

Thompson, P. M., MacDonald, D., Mega, M. S., Holmes, C. J., Evans, A. C., and Toga, A. W. 1997. Detection and mapping of abnormal brain structure with a probabalistic atlas of cortical surfaces. *J. Comput. Assist. Tomogr.* **21:** 567–581.

Watson, J. D. G., Myers, R., Frackowiak, R. S. J., Hajnal, J. V., Woods, R. P., Mazziotta, J. C., Shipp, S., and Zeki, S. 1993. Area V5 of the human brain: evidence from a combined study using positron emission tomography and magnetic resonance imaging. *Cereb. Cortex* **3:** 79–94.

Woosley, C. N., Settlage, P. H., Meyer, D. R., Sencer, W., Pinto Hamuy, T., and Travis, A. M. 1952. Patterns of localization in precentral "supplementary" motor areas and their relation to the concept of a premotor area. *Res. Publ. Assoc. Nerv. Ment. Dis.* **30:** 238–264.

Worsley, K. J., Evans, A. C., Marrett, S., and Neelin, P. 1992. Determining the number of statistically significant areas if activation in the subtracted studies from PET. *J. Cereb. Blood Flow Metab.* **12:** 900–918.

Zar, J. H. 1996. *Biostatistical Analysis.* Prentice-Hall, Upper Saddle River, NJ.

Zilles, K., Schlaug, G., Matelli, M., Luppino, G., Schleider, A., Qu, M., Dabringhaus, A., Seitz, R., and Roland, P. E. 1995. Mapping of the human and macaque sensorimotorAreas by integrating architectonic, transmitter receptor, MRI and PET data. *J. Anat.* **187:** 515–537.